Insect Biochemistry and Molecular Biology 163 (2023) 104040

Contents lists available at ScienceDirect

Insect Biochemistry and Molecular Biology

journal homepage: www.elsevier.com/locate/ibmb

Different myrosinases activate sequestered glucosinolates in larvae and adults of the horseradish flea beetle

Johannes Körnig [a,b], Kris Ortizo [a], Theresa Sporer [a], Zhi-Ling Yang [a,c], Franziska Beran [a,b,d,*]

[a] Research Group Sequestration and Detoxification in Insects, Max Planck Institute for Chemical Ecology, Jena, Germany
[b] Department Insect Symbiosis, Max Planck Institute for Chemical Ecology, Jena, Germany
[c] Xishuangbanna Tropical Botanical Garden, Chinese Academy of Sciences, Menglun, Yunnan, China
[d] Population Ecology Group, Friedrich-Schiller Universität Jena, Jena, Germany

ARTICLE INFO

Keywords:
Flea beetle
Phyllotreta
Glucosinolate
Myrosinase
Defense
Sequestration

ABSTRACT

β-Glucosidases play an important role in the chemical defense of many insects by hydrolyzing and thereby activating glucosylated pro-toxins that are either synthesized *de novo* or sequestered from the insect's diet. The horseradish flea beetle, *Phyllotreta armoraciae*, sequesters pro-toxic glucosinolates from its brassicaceous host plants and possesses endogenous *β*-thioglucosidase enzymes, known as myrosinases, for glucosinolate activation. Here, we identify three myrosinase genes in *P. armoraciae* (*PaMyr*) with distinct expression patterns during beetle ontogeny. By using RNA interference, we demonstrate that *PaMyr1* is responsible for myrosinase activity in adults, whereas *PaMyr2* is responsible for myrosinase activity in larvae. Compared to *PaMyr1* and *PaMyr2*, *PaMyr3* was only weakly expressed in our laboratory population, but may contribute to myrosinase activity in larvae. Silencing of *PaMyr2* resulted in lower larval survival in a predation experiment and also reduced the breakdown of sequestered glucosinolates in uninjured larvae. This suggests that PaMyr2 is involved in both activated defense and the endogenous turnover of sequestered glucosinolates in *P. armoraciae* larvae. In activity assays with recombinant enzymes, PaMyr1 and PaMyr2 preferred different glucosinolates as substrates, which was consistent with the enzyme activities in crude protein extracts from adults and larvae, respectively. These differences were unexpected because larvae and adults sequester the same glucosinolates. Possible reasons for different myrosinase activities in *Phyllotreta* larvae and adults are discussed.

1. Introduction

Many insects use toxic or deterrent metabolites to protect themselves from natural enemies (Beran and Petschenka, 2022; Dettner, 2015; Sugiura, 2020). To avoid autotoxicity, some insects accumulate glucosylated pro-toxins that are produced *de novo* or sequestered from the diet, and activate these enzymatically using endogenous *β*-glucosidases upon attack (Kazana et al., 2007; Pentzold et al., 2017; de Castro et al., 2019; Sporer et al., 2020; Zagrobelny et al., 2018). Sequestration of glycosylated pro-toxins has been reported in a number of herbivorous insect species that feed on plants that produce, for example, cyanogenic glucosides, glucosinolates (GSLs), or benzoxazinoid glucosides as part of their own activated chemical defense (Beran and Petschenka, 2022; Robert et al., 2017). However, the corresponding activating *β*-glucosidases have only been identified in a few insect species (Beran et al., 2014; Jones et al., 2001; Pentzold et al., 2017; Pontoppidan et al., 2001; Rahfeld et al., 2015).

Flea beetles of the genus *Phyllotreta* almost exclusively use plants of the order Brassicales as hosts (Gikonyo et al., 2019; Rheinheimer and Hassler, 2018; Vig, 2005), which are protected against non-adapted herbivores and pathogens by GSLs and activating *β*-thioglucosidase enzymes (myrosinases) (Blažević et al., 2020). GSLs are *β*-thioglucoside-*N*-hydroxysulfates with a variable amino acid-derived side chain (Agerbirk and Olsen, 2012). GSLs and their activating myrosinase enzymes are spatially separated in intact plant tissues, but come into contact upon tissue damage, resulting in GSL hydrolysis (Chhajed et al., 2019; Wittstock et al., 2016). The initial hydrolysis product is an unstable aglucone that can give rise to several degradation products, such as isothiocyanates and nitriles (Hanschen et al., 2014; Wittstock et al., 2016). Due to their high reactivity towards biological nucleophiles, isothiocyanates act as direct defense compounds, whereas the less toxic nitriles may play a role in indirect plant defense (Hanschen et al., 2014;

* Corresponding author. Research Group Sequestration and Detoxification in Insects, Max Planck Institute for Chemical Ecology, Jena, Germany.
E-mail address: fberan@ice.mpg.de (F. Beran).

https://doi.org/10.1016/j.ibmb.2023.104040
Received 14 September 2023; Received in revised form 9 November 2023; Accepted 13 November 2023
Available online 22 November 2023

Jeschke et al., 2016a, 2016b; Mumm et al., 2008). Which hydrolysis products are formed depends on various factors, including the structure of the parent GSL, the reaction conditions, and the presence of so-called specifier proteins (Eisenschmidt-Bönn et al., 2019; Wittstock et al., 2016).

Previous studies with the striped flea beetle, *Phyllotreta striolata,* and the horseradish flea beetle, *Phyllotreta armoraciae*, have shown that both species sequester ingested GSLs and possess their own myrosinases, allowing them to activate sequestered GSL for their own purposes (Beran et al., 2014; Sporer et al., 2020). While the GSL profile of the food plant strongly influenced the sequestration pattern, it had no detectable impact on myrosinase activity in *P. armoraciae* larvae (Sporer et al., 2020; Yang et al., 2020). Sequestered GSLs were found in all *P. armoraciae* life stages from eggs to adults, with significantly higher GSL concentrations detected in eggs, pupae, and adults compared to larvae (Sporer et al., 2020). In addition to the variation in GSL levels, myrosinase activity also varies between life stages, with much higher myrosinase activity in larvae and adults compared to eggs and pupae. The different levels of myrosinase activity in larvae and pupae correlated with their ability to deter a generalist predator (Sporer et al., 2020). However, GSL hydrolysis products were also detectable in bodies and feces of uninjured larvae and adults that had fed on leaves of the *tgg1*×*tgg2* double knock-out mutant of *Arabidopsis thaliana*, which has undetectable myrosinase activity in leaves. This suggests that beetle myrosinases also mediate endogenous turnover of sequestered GSLs independent of a predator attack (Sporer et al., 2021). In feeding experiments with larvae and adults, both simple nitriles and isothiocyanates were detected, indicating that different hydrolysis products are formed *in vivo* (Sporer et al., 2021).

This study aimed to identify and characterize the genes responsible for myrosinase activity in *P. armoraciae* larvae and adults. For this purpose, we focused on the glycoside hydrolase family 1 (GH1), to which all known myrosinases from both plants and insects belong (He et al., 2022). Previous research identified a total of 28 *GH1*-like genes in a transcriptome from adult *P. striolata*, one of which encoded an enzyme with myrosinase activity (Beran et al., 2014). In a phylogenetic analysis, the *P. striolata* myrosinase (PsMyr) clustered together with β-O-glucosidases involved in the chemical defense of leaf beetles of the subtribe Chrysomelina, suggesting a common origin of defensive β-glucosidases in leaf beetles (Rahfeld et al., 2015). To obtain a comprehensive GH1 dataset for *P. armoraciae*, we searched for *GH1*-like genes in the transcriptomes of larvae, pupae, and adults, and used phylogenetic analyses to identify candidate myrosinases. With this approach we found three candidate myrosinases that were characterized *in vitro*. Finally, we used RNA interference to verify the function of the identified myrosinase genes in *P. armoraciae* larvae and adults.

2. Materials and methods

2.1. Insect rearing

Phyllotreta armoraciae beetles were reared on potted *Brassica juncea* cv. Bau-Sin plants (Known-You Seeds, Kaohsiung, Taiwan) or *Brassica rapa* cv. Yu-Tsai-Sum plants (Known-You Seeds) as described earlier (Sporer et al., 2020). Adults of the generalist predator *Harmonia axyridis* were collected in Ober-Mörlen (Hesse, Germany) in spring 2021. To obtain *H. axyridis* larvae for predation experiments, we reared the beetles on pea aphids, *Acyrthosiphon pisum*, at 23 °C, 60% relative humidity and a 16:8 h light-dark period. Pea aphids were provided by Dr. Grit Kunert (Max Planck Institute for Chemical Ecology, Jena, Germany) and reared on potted *Vicia faba* cv. "The Sutton" plants.

2.2. Chemicals

4-Hydroxybenzyl GSL was isolated from *Sinapis alba* seeds following Thies (1988) and 2-propenyl GSL was purchased from Roth (Karlsruhe, Germany). All other GSLs were purchased from Phytoplan (Heidelberg, Germany). Catalpol, 4-nitrophenyl glucopyranoside (4NPG), and 4-pentenenitrile were purchased from Sigma-Aldrich (St. Louis, USA). The cyanogenic glucoside linamarin was purchased from Biozol (Eching, Germany), benzyl isothiocyanate was purchased from Thermo Fisher Scientific (Waltham, USA), benzonitrile was purchased from Merck Millipore (Darmstadt, Germany), 4-methylsulfinylbutyl isothiocyanate was purchased from Alexis Biochemicals (San Diego, USA), and phenylacetonitrile was purchased from Tokyo Chemical Industries (Tokyo, Japan).

2.3. RNA extraction, RNA sequencing and de novo transcriptome assembly

To obtain a transcriptome from immature life stages of *P. armoraciae,* we collected third instar larvae and pupae from the rearing colony. Five larvae were dissected to separate the gut including the Malpighian tubules from the residual body. Total RNA was extracted from larval guts and the residual bodies, as well as from intact larvae and pupae (pool of three individuals per life stage) using the innuPrep RNA Mini Kit 2.0 (Analytik Jena, Jena, Germany). Genomic DNA was removed using Turbo DNase (Thermo Fisher Scientific) and a final clean-up was performed using the RNeasy MinElute Cleanup Kit (Qiagen, Hilden, Germany). RNA quality was checked using a Bioanalyzer 2100 with the RNA 6000 Nano Kit (Agilent Technologies, Santa Clara, USA). Library preparation including poly-A enrichment and sequencing was performed at the Max Planck Genome Centre (Köln, Germany) using the Illumina HiSeq 3000 system in paired-end read mode (2 × 150 bp). Between 28 and 43 million reads were obtained per sample. Reads were filtered and trimmed using CLC Genomics Workbench 10.0.1. A random subset of 20% of the reads from whole larvae, larval guts, and pupae was used to assemble a transcriptome in CLC Genomics Workbench 10.0.1 with the following parameters: nucleotide mismatch cost = 1, insertion cost = 2, deletion cost = 2, length fraction = 0.6, similarity = 0.9. Contigs shorter than 200 bp were removed from the final assembly, which contained 18,079 contigs with an N50 contig size of 2649 bp.

2.4. cDNA synthesis

First-strand cDNA was synthesized from total RNA extracted from *P. armoraciae* larvae and adults (2.5 μg RNA from each life stage) using the SuperScript IV First-Strand Synthesis System (Thermo Fisher Scientific) with anchored oligo-dT primers according to the manufacturer's instructions. In addition, 5′- and 3′-rapid amplification of cDNA ends (RACE)–cDNA was synthesized using the SMARTer RACE cDNA Amplification Kit (Clontech, Mountain View, USA).

2.5. Identification, cloning, and sequencing of GH1-like genes from P. armoraciae

To obtain a comprehensive GH1 dataset from *P. armoraciae* for the identification of candidate myrosinase genes, were performed tBlastn searches with the *P. striolata* myrosinase (GenBank accession: AHZ59651.1) as a query against three different transcriptomes of *P. armoraciae*, i.e., the *de novo* assembled transcriptome from larvae and pupae (this study) and two available transcriptome assemblies from adults (Beran et al., 2016; Yang et al., 2021). To obtain the full-length sequences of partial ORFs, we performed 5′- and 3′-RACE PCR according to the manufacturer's protocols using the Advantage 2 Polymerase Mix (Clontech). Full-length ORFs were amplified from cDNA using gene-specific primers by PCR using Phusion Taq polymerase (Thermo Fisher Scientific), cloned into the pCR4-TOPO vector (Thermo Fisher Scientific), and Sanger sequenced. Primer sequences are listed in Table S1. The manually curated nucleotide sequences were submitted to GenBank under accession numbers OP313699 to OP313730 (Table S2). The corresponding amino acid sequences were used to predict the

molecular mass and isoelectric point of the proteins using the Compute pI/Mw tool (Gasteiger et al., 2005), the number of putative N-glycosylation sites using the NetNGlyc 1.0 tool (Gupta and Brunak, 2002), and the presence of a signal peptide using SignalP 5.0 (Almagro Armenteros et al., 2019).

2.6. Identification of myrosinase-like genes in genomes of P. striolata and P. cruciferae

Recently, chromosome-level genome assemblies of *P. striolata* (GenBank assembly accession: GCA_918026865.1) and *Phyllotreta cruciferae* (GenBank assembly accession: GCA_917563865.1) have been published (King et al., 2023). To search for myrosinase-like genes in these genome assemblies, we performed tBlastn searches with the amino acid sequences of PsMyr (GenBank accession: AHZ59651.1), PaMyr1 (GenBank accession: OP313699) and PaMyr2 (GenBank accession: OP313700) using the software Geneious Prime. We extracted genomic regions producing alignments with high sequence similarity and manually predicted full-length coding sequences of myrosinase-like genes in Sequencher 5.4.6 using the predicted exon-intron structure of PsMyr as a guide.

2.7. Phylogenetic analyses of putative GH1 β-glucosidases from Phyllotreta spp.

The GH1-like protein sequences from *P. armoraciae* were aligned with the published GH1 dataset from *P. striolata* (GenBank accession numbers: KF377828 to KF377855), four myrosinase-like sequences identified in the genomes of *P. striolata* and *P. cruciferae,* and the *Brevicoryne brassicae* aphid myrosinase (GenBank accession: Q95X01.1) as outgroup using MAFFT version 7 with default settings (Katoh et al., 2019). Poorly aligned regions were eliminated using Gblocks version 0.91b (Talavera and Castresana, 2007) with parameters set as follows: minimum length of 5 amino acids for a block after cleaning, minimum of 33 sequences for a conserved position, minimum of 33 sequences for a flank position, maximum of 8 contiguous non-conserved positions, and half of gap positions allowed. Maximum Likelihood phylogenetic analyses were inferred using IQ-TREE version 1.6.12 (Nguyen et al., 2015). The LG + I + G4 model was determined as the best-fit substitution model using ModelFinder implemented in IQ-TREE (Kalyaanamoorthy et al., 2017). Branch supports were assessed using an ultrafast bootstrap approximation with 10,000 replicates (Hoang et al., 2018).

Bayesian phylogenetic analysis of the same dataset was conducted using MrBayes 3.2.7a using the LG + I + G4 substitution model with two runs, each with six heated and two cold Markov chains (Huelsenbeck and Ronquist, 2001; Ronquist et al., 2012). Chains were sampled every 100,000 generations and analyses were continued until the runs converged, which happened after six million generations. The first 25% of trees were discarded as burn-in. Analyses was performed on CIPRES Science Gateway (Miller et al., 2010).

2.8. Cloning and expression of myrosinase candidate genes

Full-length ORFs of *PaMyr1*, *PaMyr2*, *PaMyr3,* and *PaGH1-28* were amplified from *P. armoraciae* cDNA by PCR (Phusion High-Fidelity DNA Polymerase, Thermo Fisher Scientific) and cloned into the pIEx-4 expression vector (Merck Millipore), using gene-specific primers (Table S1). The reverse primer lacked the native stop codon for C-terminal fusion to the vector-encoded His_8-tag. Expression constructs confirmed by Sanger-sequencing were used to transiently transfect High Five insect cells (Thermo Fisher Scientific). High Five cells were cultivated in Express Five SFM medium (Gibco, Thermo Fisher Scientific) supplemented with 20 mM glutamine (Gibco) and 50 μg ml^{-1} gentamycin (Gibco). Confluent cells were diluted 1:5 and dispensed in 500 μl aliquots into a 24-well plate. After incubation at 27 °C for 6–12 h, cells were transfected using FuGENE HD Transfection Reagent (Promega, Madison, USA) according to the manufacturer's protocol. Cells treated only with transfection reagent served as negative controls. Cell culture medium was harvested after incubation at 27 °C for 72 h and centrifuged (5 min at 16,000 g and 4 °C) to remove cell debris. Recombinant proteins were detected by Western blotting using the Anti-His (C-Term)-HRP antibody (1:20,000, Novex, Thermo Fisher Scientific). The cell culture medium containing the recombinant enzymes was dialyzed against 2-(N-morpholino)-ethanesulfonic acid (MES) buffer (20 mM, pH 6.5) using slide-A-Lyzer Dialysis cassettes with a molecular weight cut-off of 10,000 kDa (Extra strength, Thermo Fisher Scientific).

2.9. Biochemical characterization of candidate myrosinases

Activity of recombinant GH1 enzymes with different GSLs, the iridoid glucoside catalpol, the cyanogenic glucoside linamarin, and the general substrate 4NPG was determined using the Amplite Fluorimetric Glucose Quantitation Kit (AAT Bioquest, Pleasanton, USA). Enzyme assays were performed at 24 °C in dark 96-well plates and consisted of 25 μl protein sample, 25 μl substrate (each at 2 mM, dissolved in 20 mM MES buffer, pH 6.5), and 50 μl assay reagent. To determine the K_M values for 2-propenyl GSL, assays were performed with substrate concentrations ranging from 0.01 to 10 mM. Assays with boiled protein served as background control. All assays were performed in triplicates. Fluorescence intensity (Ex/Em = 540 nm/590 nm) was monitored every minute for 30 min using an Infinite 200 Reader (Tecan, Männedorf, Switzerland). Glucose amounts in each assay were calculated using a glucose standard curve (dissolved in MES buffer, pH 6.5) for each time point. K_M values were estimated by nonlinear regression analysis in R using drm() (Ritz et al., 2015) based on the Michaelis-Menten equation for single-substrate reaction and the Haldane equation for single-substrate inhibition of enzymatic reaction rate (Haldane, 1930; Sonnad and Goudar, 2004).

2.10. Biochemical characterization of myrosinase activity in larvae and adults

To compare the substrate specificity of myrosinase activity in larvae with that in adults, we prepared crude protein extracts from third instar larvae and seven-day-old adults that had been fed with *B. juncea* leaves. Samples were weighed, frozen in liquid nitrogen, and stored at −80 °C until extraction ($N = 3$ per life stage, 10 individuals per replicate). For protein extraction, samples were homogenized in ice-cold MES buffer (20 mM, pH 6.5) containing protease inhibitors (cOmplete, EDTA-free, Roche, Basel, Switzerland) using metal beads (2 mm diameter) for 2 min at 25 Hz in a TissueLyser II (Qiagen) and centrifuged (5 min at 16,000 g at 4 °C). To remove GSLs and other small molecules that interfere with enzyme activity from the crude extract, we applied the supernatant first to a 7 mg DEAE-Sephadex A-25 column (GE Healthcare, Chicago, USA) and subsequently to a 0.5 ml Zeba Spin Desalting Column (molecular weight cut-off: 7 kDa; Thermo Fisher Scientific). Both columns were equilibrated with MES buffer containing protease inhibitors before loading the protein extract. The total concentration of soluble protein was determined using the Bradford protein assay (Bio-Rad, Hercules, USA). For our enzyme assays, we diluted the crude protein extracts to 2.5 μg ml^{-1} in MES buffer. Enzyme assays with different substrates and different concentrations of 2-propenyl GSL were performed as described in the previous section, with two technical replicates. Assays without substrate and without protein served as background controls.

2.11. Impact of Fe(II) ion on formation of glucosinolate hydrolysis products

To determine how GSL structure and the presence of Fe(II) ion influence the composition of hydrolysis products, namely isothiocyanates and simple nitriles, we incubated recombinant PaMyr1, PaMyr2, and

PaMyr3 and mock-transfected control samples with either 3-butenyl GSL or benzyl GSL in the presence or absence of Fe(II) ion. We used 3-butenyl GSL instead of 2-propenyl GSL because the simple nitrile derived from 2-propenyl GSL could not be detected under our analytical conditions. However, all three recombinant PaMyr enzymes showed similar activities with 2-propenyl GSL and 3-butenyl GSL under our assay conditions. Each recombinant enzyme was assayed with 0.5 mM GSL substrate and 50 mM EDTA or 0.5 mM $FeSO_4$ in 100 µL MES buffer (20 mM, pH 6.5). Assays were overlaid with 100 µl hexane containing benzonitrile (1:100,000). After incubation at 27 °C for 30 min, hydrolysis products were extracted by vigorous mixing for 5 min. To separate the organic from the aqueous phase, samples were centrifuged (10 min at 6000 g at room temperature), frozen in liquid nitrogen, set to room temperature, and the hexane fraction was collected while the aqueous phase was still frozen. Assays with dialyzed medium of non-transfected cells and assays without substrate served as background controls.

Hydrolysis products were identified by gas chromatography-mass spectrometry (GC-MS) using an Agilent 6890 instrument equipped with an OPTIMA 5 capillary column (30 m × 0.25 mm i.d. × 0.25 µm film thickness; Macherey-Nagel, Düren, Germany) coupled to a 5973 quadrupole mass spectrometer (Agilent Technologies). The carrier gas was helium at a constant flow rate of 1 ml min^{-1}. One microliter per sample was injected in splitless mode. The front inlet temperature was set to 200 °C. The oven program started at 45 °C (held for 3 min), increased at 10 °C min^{-1} to 220 °C, and then with 70 °C min^{-1} to 300 °C (held for 3 min). Mass spectrometry conditions were electron impact mode (70 eV), and scan mode m/z 33–260. Hydrolysis products were identified in comparison to authentic standards and published MS spectra (Spencer, 1980).

Hydrolysis products were quantified using gas chromatography coupled with flame ionization using an Agilent 6890 instrument equipped with an Optima 5 capillary column (see above). The carrier gas was helium and the detector temperature was 300 °C. The injection conditions and oven program were identical to the conditions described above. FID response factors of hydrolysis products relative to the internal standard benzonitrile were calculated using the effective carbon number concept (Scanlon and Willis, 1985). Traces of hydrolysis products found in non-transfected controls were subtracted as background.

2.12. Myrosinase activity and PaMyr transcript levels in different life stages of P. armoraciae

To better understand the role of the different *PaMyr* genes in *P. armoraciae*, we compared myrosinase activity in different life stages with *PaMyr* transcript levels. Therefore, we collected eggs, larvae (first, second, third instar, and prepupal stage), pupae, seven days-old adult females, and seven days-old adult males from the rearing colony. For protein extraction, samples were weighed, frozen in liquid nitrogen, and stored at −80 °C (N = 6–7 per life stage). Crude protein extracts were prepared as described in section 2.10 and myrosinase activity assays were performed as described in section 2.9 using 125 ng total protein and 0.5 mM 2-propenyl GSL as substrate. For RNA extraction, samples were homogenized in lysis buffer (InnuPREP RNA Mini Kit 2.0, Analytik Jena) for 2 min at 25 Hz in a TissueLyzerII (Qiagen) using metal beads, frozen in liquid nitrogen, and stored at −80 °C (N = 6 per life stage). Total RNA was extracted using the InnuPREP RNA Mini Kit 2.0 (Analytik Jena), genomic DNA was removed with TURBO DNase (Thermo Fisher Scientific), and RNA was purified using the RNeasy MinElute Cleanup Kit (Qiagen). RNA concentration was determined using a N60 spectrophotometer (Implen, München, Germany) and cDNA was prepared with the Verso cDNA Synthesis Kit (Thermo Fisher Scientific) from 800 ng total RNA using anchored oligo-dT and random hexamer primers in a ratio of 1:3. Transcript levels of *PaMyr1*, *PaMyr2*, and *PaMyr3* were analyzed by quantitative PCR (qPCR) using gene-specific primers (Table S1) in optical 96-well plates on a CFX Connect Real-Time-System (Bio-Rad) using the Absolute Blue qPCR SYBR Green Kit (Thermo Fisher Scientific). The PCR program was as follows: 95 °C for 15 min, 40 cycles of 95 °C for 15 s, 57 °C for 30 s and 72 °C for 30 s. Afterwards, the melting curve was determined from 55 °C to 95 °C in 0.5 °C increments. Primer efficiencies were calculated using a cDNA template dilution series. Transcript levels were normalized to the transcript level of the reference gene that showed the lowest variability across life stages among several tested reference genes, i.e., ribosomal protein 18a, ribosomal protein L32e, and eukaryotic initiation factor-4A, 40S ribosomal protein subunit 4.

Myrosinase activity and transcript levels were compared among life stages using the generalized least squares method using gls() from the nlme library (Pinheiro et al., 2021) in R3.3.1 (R Core Team, 2023). We applied a constant variance function structure (varIdent) implemented in the nlme library in R, which allows each life stage to have a different variance. *P*-values and log likelihood values were obtained by removing the explanatory variable and comparing models with likelihood ratio tests (Zuur, 2009). Significant differences between life stages were determined by post hoc multiple comparison of estimated means using Tukey contrasts (glht from the multcomp library (Hothorn et al., 2020), Table S3).

2.13. Silencing of PaMyr1 and PaMyr2 by RNA interference

Double stranded RNA (dsRNA) targeting *PaMyr1* (158 bp), *PaMyr2* (225 bp), or a lepidopteran metalloproteinase inhibitor (*IMPI*) from *Galleria mellonella* (GenBank accession: AY330624.1; 223 bp) was synthesized using the T7 RiboMAX Express RNAi System (Promega). Putative off-targets were identified by searching all possible 21-mers of both RNA strands against our *P. armoraciae* transcriptomes allowing for two mismatches. Several *PaGH1* transcripts were identified as putative off-targets of *dsPaMyr1* and *dsPaMyr2*, of which *PaMyr3* is the most likely to be affected based on mismatch number (Table S4).

One day after eclosion, adults were injected with 100 nl ultrapure water containing 80 ng dsRNA targeting *PaMyr1* or *IMPI* as a control. Injected adults were kept in the laboratory under ambient conditions with detached *B. juncea* leaves as a food source. Seven days after injection, adults were sampled to determine myrosinase activity (N = 8 per treatment, 2 adults per sample), transcript levels (N = 7 per treatment, 1 adult per sample), and GSL concentration (N = 12 per treatment, 1 adult per sample).

Second instar larvae were injected with 50 nl ultrapure water containing 80 ng dsRNA targeting *PaMyr2* or *IMPI* as a control. Injected larvae were provided with *B. juncea* leaf petioles and kept in the laboratory under ambient conditions. Six days after injection, third instar larvae were sampled to determine myrosinase activity assays (N = 8 per treatment, 3 larvae per sample), transcript levels (N = 7 per treatment, 3 larvae per sample), and GSL concentration (N = 7 per treatment, 3 larvae per sample). Protein extraction, myrosinase activity assays, RNA extraction, cDNA synthesis, and qPCR analyses were performed as described above. GSLs were extracted, converted to desulfo-GSLs, and analyzed using high performance liquid chromatography coupled to diode array detection (HPLC-DAD) as described in Beran et al. (2014). *PaMyr* transcript levels, myrosinase activities, and GSL concentrations were compared with *t*-tests or Mann-Whitney Rank sum tests in R3.3.1 (R Core Team, 2023) or in SigmaPlot 11.0 (Systat Software; Table S3).

2.14. Predation assay

To determine whether myrosinase activity protects *P. armoraciae* larvae against a generalist predator, we exposed *PaMyr2*-silenced *P. armoraciae* larvae and *dsIMPI* injected control larvae to *H. axyridis*. dsRNA injections were performed on three consecutive days, with at least 13 replicates per treatment and day. Six days after injection, samples were collected to confirm that *PaMyr2*-silencing was successful (*PaMyr* transcript levels and myrosinase activity, N = 7–8 per treatment, 2 larvae per sample). We then monitored larval survival as described

previously in Sporer et al. (2020). In brief, one *P. armoraciae* larva and one *H. axyridis* third instar larva were placed in a Petri dish (60 mm diameter). Survival of *P. armoraciae* larvae was recorded in 30 min intervals for 6 h ($N = 68–72$ per treatment). Assays in which *H. axyridis* larvae had molted or died were excluded from the analysis. Survival data were analyzed using a parametric survival regression model with a lognormal hazard distribution in R3.3.1 (Therneau, 2020). The effect of dsRNA treatment and day of the experiment was evaluated using log-rank tests (Table S3).

2.15. Feeding assay

To determine whether *PaMyr2* is also involved in endogenous metabolism of sequestered GSL in larvae, we performed a feeding assay with the *A. thaliana tgg1×tgg2* mutant, which is devoid of myrosinase activity in leaves (Barth and Jander, 2006), and contains mainly 4-methylsulfinylbutyl GSL (4MSOB GSL), which is not present in *P. armoraciae* larvae reared on *B. juncea*. *Arabidopsis* plants were cultivated at 21 °C, 60% relative humidity under short-day conditions (10:14 h light-dark) in a controlled environment chamber. *PaMyr2*-silenced and *dsIMPI* injected control larvae were allowed to feed on a detached leaf of an *A. thaliana tgg1×tgg2* mutant plant ($N = 12$ per treatment, 4 larvae per replicate). We removed the major leaf vein to prevent larvae from mining. After one day, feces were collected in 50 µl 0.1% (v/v) formic acid in ultrapure water, mixed with 50 µl pure methanol and homogenized for 2 min at 25 Hz in a TissueLyzerII (Qiagen) using metal beads. Larvae were weighed and frozen in liquid nitrogen. All samples were stored at −20 °C until extraction. Larvae were homogenized in 500 µl ice-cold 50% (v/v) methanol for 2 min at 25 Hz in a TissueLyzerII (Qiagen) using metal beads. Homogenized body and feces samples were centrifuged (10 min at 16,000 g at 4 °C), and supernatants were transferred to new glass vials and stored at −20 °C until analysis by liquid chromatography coupled with tandem mass spectrometry (LC-MS/MS). To confirm silencing of *PaMyr2*, samples for qPCR ($N = 6–7$ per treatment, 3 larvae per sample) and myrosinase activity assays ($N = 8$ per treatment, 3 larvae per sample) were collected and analyzed as described above. We quantified the amounts of 4MSOB GSL, 4MSOB-isothiocyanate (4MSOB-ITC), 4MSOB-cyanide, and 4MSOB-amine in body and feces extracts, and calculated the proportion of hydrolysis products relative to the amounts of GSLs and derived hydrolysis products. The relative proportions of hydrolysis products were compared between treatments with *t*-tests or Mann-Whitney Rank sum tests in R3.3.1 (R Core Team, 2023) or in SigmaPlot 11.0 (Systat Software; Table S3).

2.16. LC-MS/MS analysis

4MSOB GSL and corresponding hydrolysis products were quantified by LC-MS/MS using an Agilent 1200 HPLC system connected to an API3200 tandem mass spectrometer (AB Sciex, Framingham, USA) using external standard curves for 4MSOB GSL and the corresponding isothiocyanate. Other 4MSOB GSL-derived hydrolysis products were quantified using relative response factors towards 4MSOB-ITC.

Intact GSLs were separated on a Nucleodur Sphinx RP column (250 × 4.6 mm, 5 µm particle size; Macherey-Nagel) using a mobile phase consisting of 0.2% (v/v) formic acid in ultrapure water as solvent A and acetonitrile as solvent B, at a flow rate of 1 ml min^{-1}. The gradient was as follows: 1.5% (v/v) B (1 min), 1.5–5% (v/v) B (5 min), 5–7% (v/v) B (2 min), 7–13.3% (v/v) B (4.5 min), 13.3–100% (v/v) B (0.1 min), 100% B (0.9 min), 100–1.5% (v/v) B (0.1 min), 1.5% (v/v) B (3.9 min). The presence of GSLs was detected with the ionization source set to negative mode. Ionspray voltage was maintained at −4500 eV. Gas temperature was set to 700 °C, nebulizing gas to 70 psi, drying gas to 60 psi, curtain gas to 20 psi, and collision gas to 10 psi.

Hydrolysis products of 4MSOB GSL were separated on a Zorbax Eclipse XDB-C18 column (50 × 4.6 mm, 1.8 µm particle size; Agilent Technologies) using a mobile phase consisting of 0.05% (v/v) formic acid in ultrapure water as solvent A and acetonitrile as solvent B, at a flow rate of 1.1 ml min^{-1}. Separation of 4MSOB GSL hydrolysis products was achieved by using the following gradient: 3–15% (v/v) B (0.5 min), 15–85% (v/v) B (2 min), 85–100% (v/v) B (0.1 min), 100% B (0.9 min) 100–3% (v/v) B (0.1 min), 3% (v/v) B (2.4 min). The ionspray voltage was maintained at 5500 eV. The gas temperature was set to 650 °C. Nebulizing gas was set at 60 psi, curtain gas at 35 psi, heating gas at 60 psi, and collision gas at 4 psi. Multiple-reaction monitoring was used to monitor analyte parent ion-to-product ion formation (Table S5). Data analysis was performed using Analyst Software 1.6 Build 3773 (AB Sciex).

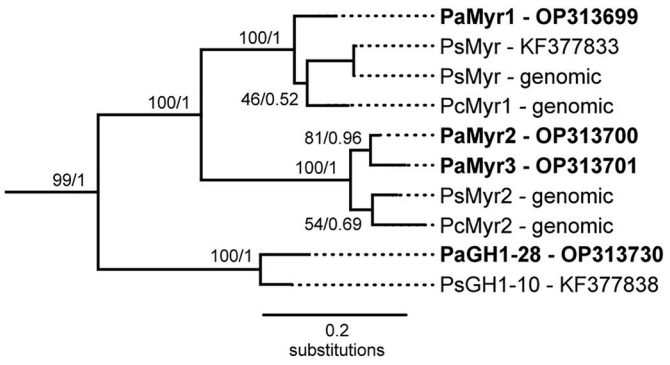

Fig. 1. Maximum-likelihood phylogeny of *Phyllotreta* myrosinases and the most closely related GH1 enzymes. The complete phylogeny of GH1 enzymes from *Phyllotreta* spp. is shown in Fig. S1. Bootstrap values (10,000 replicates) and posterior probability values of a Bayesian analysis using the same dataset are shown next to each node. Enzymes from *P. armoraciae* (Pa) that were characterized in this study are shown bold. Candidate myrosinases from *P. striolata* (Ps) and *P. cruciferae* (Pc) identified in publicly available genome assemblies are labeled "-genomic".

2.17. Glucosinolate composition in different life stages of P. armoraciae

To determine whether the GSL sequestration pattern differs between different life stages of *P. armoraciae*, we analyzed the GSL composition in third instar larvae, pupae, and 8-days old adults reared on *B. rapa*, which contains more diverse GSL than *B. juncea*. Fed adults were starved for one day before sampling. Larvae were sampled immediately because of high mortality under starvation conditions. Samples were weighed, frozen in liquid nitrogen, and stored at −20 °C until GSL extraction ($N = 20$). Feeding damaged *B. rapa* leaf discs (16 mm diameter, eight leaf discs per sample, $N = 6$) were collected, weighed, frozen in liquid nitrogen, freeze dried, and stored at −20 °C until GSL extraction ($N = 6$). GSLs were extracted, converted to desulfo-GSLs, and analyzed using HPLC-DAD as described in Beran et al. (2014).

For comparison, we calculated the percentage of each individual GSL relative to the total GSL concentration in each sample (set to 1). GSL proportions were normalized by sum, log-transformed, and auto scaled using MetaboAnalyst 5.0 (Pang et al., 2021) (https://www.metaboanalyst.ca/). Transformed data were analyzed by permutational multivariate ANOVA (PERMANOVA) with 9999 permutations based on Mountford distances using adonis2() from the Vegan library (Oksanen et al., 2022). Post hoc pairwise comparisons were performed with PERMANOVA using pairwise.perm.manova() with Pillai's trace criterion from the BiodiversityR package (Kindt and Coe, 2005). Obtained *P*-values were adjusted using Benjamini and Yekutieli method to control for false discovery rates (Benjamini and Yekutieli, 2001).

3. Results

3.1. P. armoraciae possesses three myrosinases

To obtain a comprehensive dataset for the identification of candidate

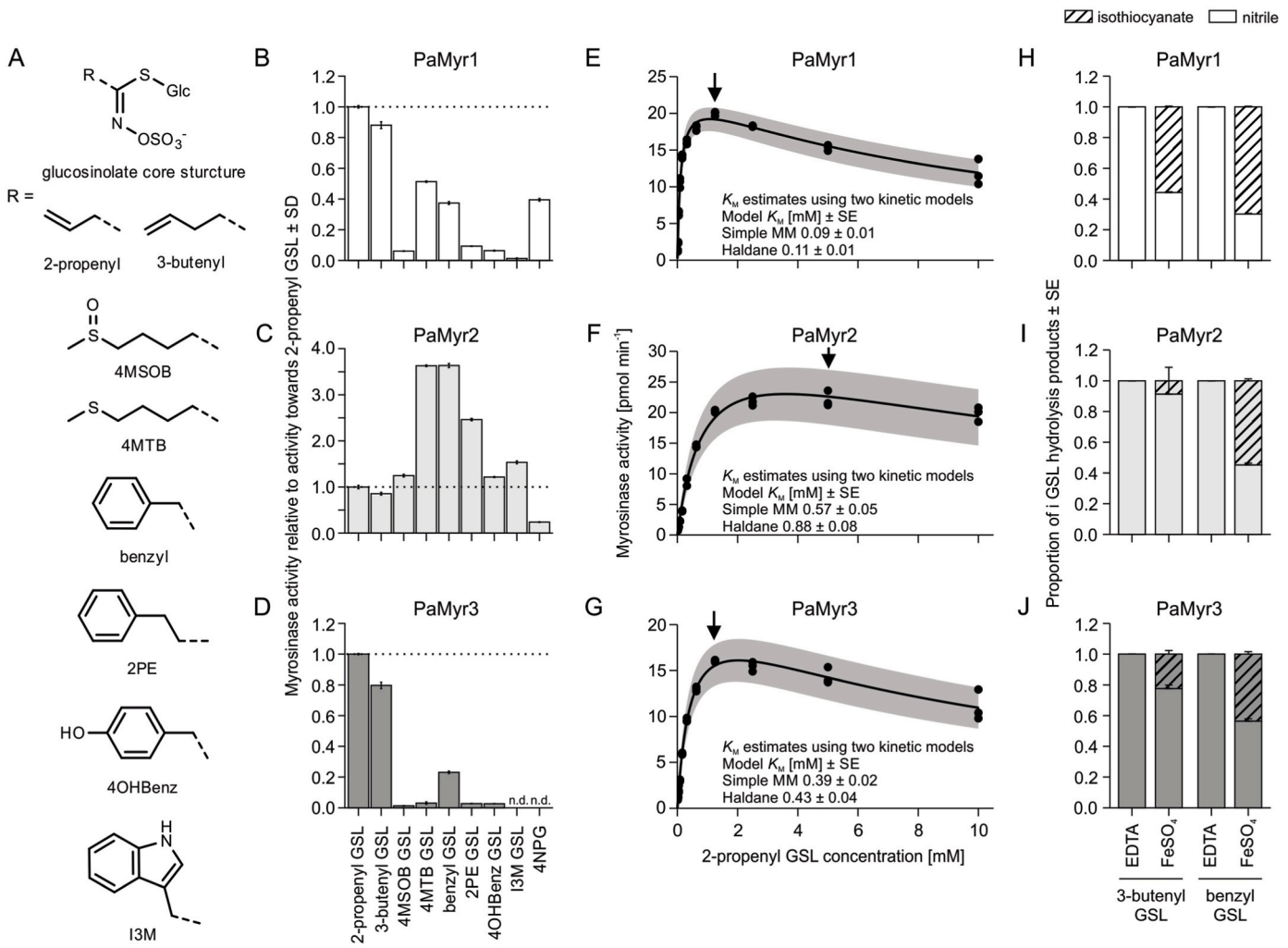

Fig. 2. Biochemical characterization of recombinant His_8-PaMyr enzymes. PaMyr1, PaMyr2, and PaMyr3 were heterologously expressed in insect cells with a C-terminal His_8-tag and incubated with different substrates. **(A)** Chemical structures of glucosinolates (GSLs) used in *in vitro* assays. **(B–D)** Myrosinase activity towards different GSLs and the general β-O-glucosidase substrate 4-nitrophenyl glucopyranoside (4NPG). Enzyme activity is expressed relative to activity with 2-propenyl GSL, which was set to 1 (indicated with a dotted line). All assays were performed at 24 °C and carried out in triplicates. Means and SD are shown. **(E–G)** Kinetic analysis of PaMyr activity towards 2-propenyl GSL. K_M values were determined based on two different equations. Lines show nonlinear regression used to determine K_M values based on the Haldane model for single-substrate inhibition ($R^2 > 0.98$ for all myrosinases). Gray bands show 95% confidence intervals. Arrows indicate the highest 2-propenyl GSL concentration used in nonlinear regression to determine the K_M values based on the Michaelis-Menten model (Simple MM). **(H–J)** Relative composition of isothiocyanate and nitrile hydrolysis products detected in enzyme assays with recombinant PaMyr1, PaMyr2, or PaMyr3 using 3-butenyl GSL or benzyl GSL as substrates. Assays were performed in the presence of 50 mM EDTA or 0.5 mM $FeSO_4$ at pH 6.5. Hydrolysis products were quantified using gas chromatography coupled with flame ionization detection. The proportions of isothiocyanate and nitrile hydrolysis products are expressed relative to the total amount of detected hydrolysis products (set to 1). n.d., not detected; 4MSOB, 4-methylsulfinylbutyl; 4MTB, 4-methylthiobutyl; 2 PE, 2-phenylethyl; 4OHBenz, 4-hydroxybenzyl; I3M, indol-3-ylmethyl.

myrosinases in *P. armoraciae*, we searched for *GH1*-like sequences in transcriptomes of this species. In total, we recovered 32 *GH1*-like genes (Table S2; GenBank accession numbers OP313699 to OP313730). We then analyzed the phylogenetic relationships among the predicted GH1 proteins from *P. armoraciae* and *P. striolata*. The result suggests that most *GH1* genes in both species evolved from common ancestors and are therefore true orthologues (Fig. S1). An exception was found in the clade containing the known *P. striolata* myrosinase (PsMyr), where three predicted GH1 proteins from *P. armoraciae* clustered together with PsMyr, suggesting a lineage-specific expansion of myrosinase-like genes in *P. armoraciae* (Fig. 1).

To test whether the proteins are indeed myrosinases, we heterologously expressed them in insect cells with a C-terminal His_8-tag. All three recombinant enzymes hydrolyzed 2-propenyl GSL in enzyme assays, confirming that they have myrosinase activity. We thus named these genes *PaMyr1*, *PaMyr2*, and *PaMyr3*. The closely related *PaGH1-28* was also expressed in insect cells, but the recombinant protein did not hydrolyze 2-propenyl GSL in our enzyme assays (Fig. S2).

Because it was surprising that no homologues of *PaMyr2* and *PaMyr3* were found in an earlier study with *P. striolata* (Beran et al., 2014), we searched for additional myrosinase-like genes in recently published genome assemblies of *P. striolata* and *Phyllotreta cruciferae* (King et al., 2023). *PsMyr* was found in tandem with another gene with high sequence similarity to *PaMyr2/PaMyr3* on chromosome 4 (accession number OU900097.1 from 7,231,627 to 7,233,624 bp and from 7,233,977 bp to 7,235,817 bp). In addition, we found two adjacent myrosinase-like genes in the *P. cruciferae* genome (chromosome 5, accession number: OU830610.1 from 1,049,770 to 1,051,735 bp and from 1,052,048 to 1,053,925 bp).

In our phylogenetic analyses, the myrosinases and myrosinase-like sequences from *Phyllotreta* spp. formed two well-supported clades (both with bootstrap support = 100, posterior probability = 1; Fig. 1).

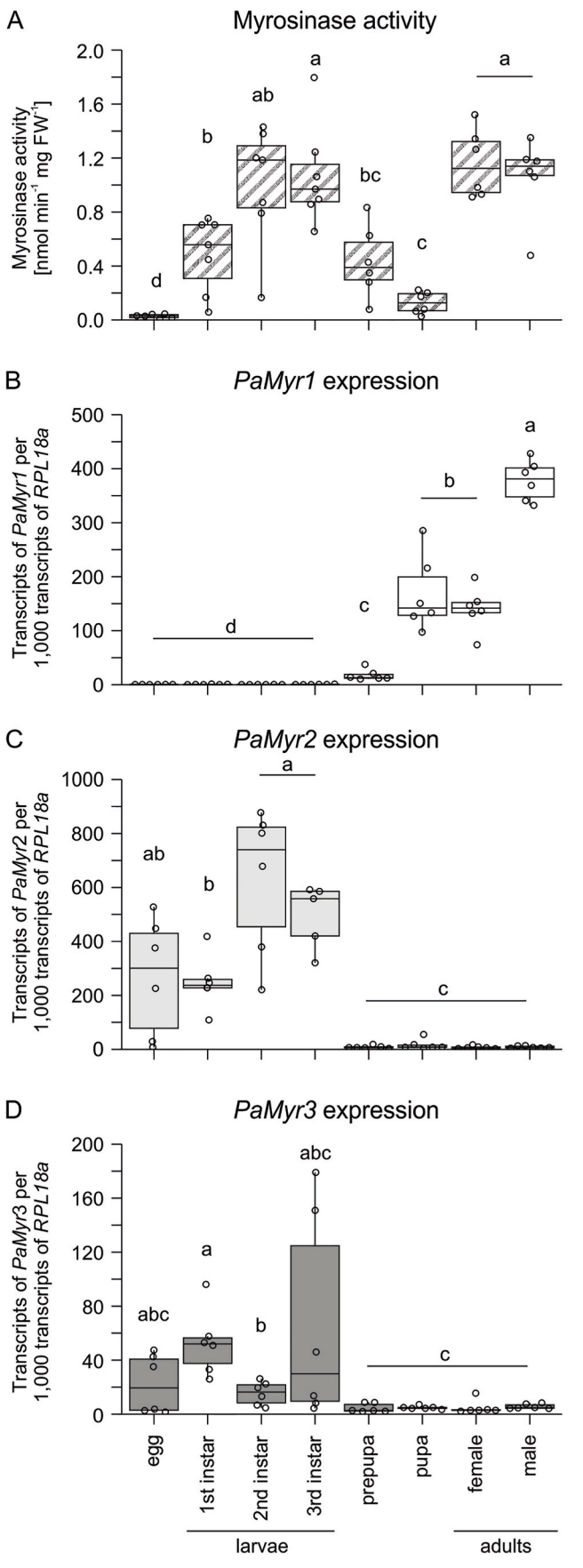

(caption on next column)

Fig. 3. Myrosinase activity and *PaMyr* transcript levels in different life stages of *P. armoraciae*. **(A)** To measure myrosinase activity, crude protein extracts were incubated with 0.5 mM 2-propenyl glucosinolate as substrate at 24 °C ($N = 6$–7 per life stage). **(B–D)** Transcript levels of *PaMyr1*, *PaMyr2*, and *PaMyr3* in different life stages were analyzed by qPCR ($N = 6$ per life stage). Copy number estimates are given per 1000 copies of the reference gene ribosomal protein L18a (*RPL18a)*. Box plots show the median and interquartile range of each dataset. Different letters indicate differences between groups ($P < 0.05$).

One clade contained PsMyr, PaMyr1 and one predicted myrosinase from *P. cruciferae*. In the second clade, PaMyr2 and PaMyr3 formed a sister group to a myrosinase-like protein from *P. striolata* and *P. cruiferae*, suggesting that *PaMyr2* and *PaMyr3* arose from a gene duplication event in the *P. armoraciae* lineage.

3.2. *PaMyr enzymes have different biochemical properties*

To compare the substrate specificities of the recombinant His_8-PaMyr enzymes, we tested their activities with eight different GSLs. Five of these GSLs (2-propenyl GSL, 3-butenyl GSL, 4-methylsulfinylbutyl GSL, 2-phenylethyl GSL, and indol-3-ylmethyl GSL) are commonly found in horseradish (Agneta et al., 2014; Ciska et al., 2017; Li and Kushad, 2004), while the remaining GSLs are found in several other brassicaceous plant species. Recombinant PaMyr1 and PaMyr3 showed similar substrate specificities and had the highest catalytic activities with 2-propenyl GSL and 3-butenyl GSL (Fig. 2B and D). Compared to recombinant PaMyr1 and PaMyr3, recombinant PaMyr2 showed a different substrate specificity and had the highest catalytic activities with benzyl GSL and 4-methylthiobutyl GSL, two GSLs that are not common in horseradish (Fig. 2C).

The recombinant PaMyr enzymes not only differed in substrate specificity, but also with respect to their Michaelis-Menten constants (K_M), for 2-propenyl GSL, the main substrate of the beetle myrosinases *in vivo*. Recombinant PaMyr1 had a lower K_M for 2-propenyl GSL (K_M value: 0.09 mM) than PaMyr2 and PaMyr3 (K_M values: 0.57 mM and 0.39 mM, respectively, Fig. 2E, F, and G). All three recombinant enzymes also showed substrate inhibition, in case of PaMyr1 and PaMyr3 at concentrations above 1.25 mM and in case of PaMyr2 at concentrations above 5 mM. At 10 mM substrate concentration, catalytic activity of PaMyr1 was reduced by 40%, activity of PaMyr2 was reduced by 10%, and activity of PaMyr3 was reduced by 31%, relative to the highest catalytic activity of the corresponding recombinant enzyme. Given that sequestered GSLs and myrosinases are co-localized in the hemolymph (Sporer et al., 2020), it is likely that myrosinase activity is inhibited by high substrate concentrations in the hemolymph (>20 mM in larvae (Sporer et al., 2020), and up to 100 mM in the hemolymph of adults (Yang et al., 2021)).

In addition to assays with GSLs, we tested enzyme activities with the general β-O-glucosidase substrate 4NPG and two other defensive plant O-glucosides, the iridoid glucoside catalpol and the cyanogenic glucoside linamarin. Only PaMyr1 and PaMyr2 hydrolyzed the general substrate 4NPG (Fig. 2B–D), showing that both enzymes have also β-O-glucosidase activity, but none of the three recombinant enzymes hydrolyzed catalpol or linamarin under our assay conditions (data not shown).

Previous experiments with *P. armoraciae* larvae and adults suggested that sequestered GSLs are converted to isothiocyanates or nitriles *in vivo* (Sporer et al., 2021). We therefore analyzed whether the presence of Fe (II) ion influences the hydrolysis of 3-butenyl GSL or benzyl GSL into the corresponding isothiocyanates and nitriles. Nitriles were only detected in enzyme assays with Fe(II) ion, with proportions ranging from 9 to 70% of the total detected hydrolysis products. The relative composition of hydrolysis products in enzyme assays with PaMyr1 differed from that in assays with PaMyr2 and PaMyr3, which responded similarly to the different conditions (Fig. 2H–J).

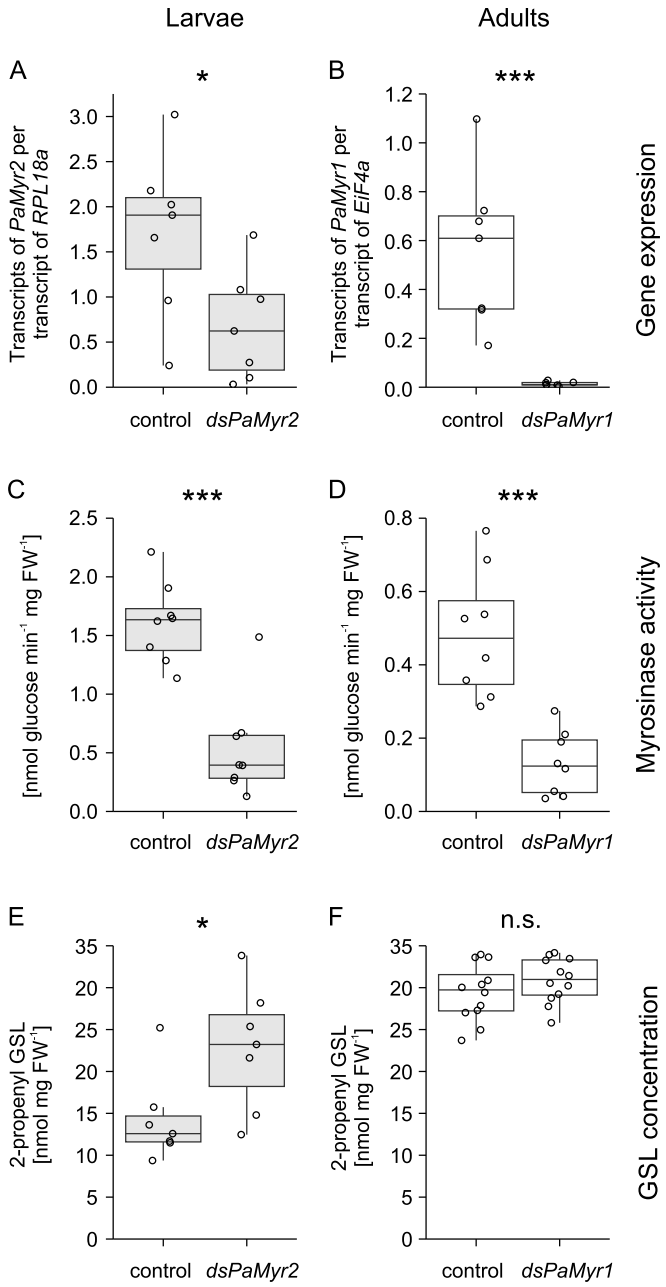

Fig. 4. Functional characterization of *PaMyr1* and *PaMyr2 in vivo*. *PaMyr1* gene expression was silenced in adults (*dsPaMyr1*) and *PaMyr2* gene expression was silenced in larvae (*dsPaMyr2)* by injecting dsRNAs. Injections of adults and larvae with dsRNA targeting a lepidopteran metalloproteinase inhibitor from *Galleria mellonella* served as controls. **(A)** *PaMyr2* transcript levels in larvae ($N = 7$). (**B**) *PaMyr1* transcript levels in adults ($N = 7$). **(C)** Myrosinase activity in larvae ($N = 8$). **(D)** Myrosinase activity in adults ($N = 8$). (**E**) Concentration of 2-propenyl glucosinolate (GSL) in larvae ($N = 7$). **(F)** Concentration of 2-propenyl glucosinolate (GSL) in adults ($N = 12$). Box plots show the median and interquartile range of each dataset. ***, $P < 0.001$; *, $P < 0.05$; n.s., not significant.

3.3. PaMyr genes are differentially expressed during the life cycle of P. armoraciae

To better understand the role of the different *PaMyr* genes in *P. armoraciae*, we compared their transcript levels in different life stages with the corresponding levels of myrosinase activity in crude protein extracts. Consistent with Sporer et al. (2020), larvae and adults showed much higher myrosinase activity than eggs and pupae (Fig. 3A; for results of statistical analyses refer to Table S3). *PaMyr1* was found to be expressed mainly in pupae and adults, while *PaMyr2* and *PaMyr3* were expressed mainly in eggs and larvae (Fig. 3B–D). However, *PaMyr2* transcripts were found to be at least five times more abundant than *PaMyr3* transcripts. Notably, *PaMyr* transcript levels did not correlate with myrosinase activity in beetle life stages. For example, we found similar levels of *PaMyr1* transcript in pupae and adults, but high myrosinase activity was detected only in adults. Nevertheless, these results suggest that *PaMyr1* is responsible for myrosinase activity in adults, whereas *PaMyr2* and to a lesser extent *PaMyr3* are responsible for myrosinase activity in larvae. This hypothesis is supported by the results of enzyme assays with crude protein extracts from adults and larvae, which showed similar substrate specificities and K_M values for 2-propenyl GSL as recombinant PaMyr1 and PaMyr2, respectively (Fig. 2, Fig. S3).

3.4. P. armoraciae larvae and adults use distinct myrosinases

To determine if indeed adults and larvae use distinct myrosinases, we silenced *PaMyr1* expression in adults and *PaMyr2* expression in larvae using RNA interference. Because *PaMyr3* is expressed at a very low level in larvae in our laboratory population, we did not attempt to silence expression of this gene. Expression of target genes was significantly reduced compared to the corresponding controls in both life stages (Fig. 4A and B, Table S3), whereas the expression levels of non-target myrosinase genes did not differ between treatments (Fig. S4, Table S3). Silencing of *PaMyr1* expression in adults and *PaMyr2* expression in larvae reduced myrosinase activities by more than 65% compared to the corresponding controls (Fig. 4C and D, Table S3). In addition, *PaMyr2*-silenced larvae contained significantly more sequestered GSL than control larvae, whereas GSL levels in adults did not differ between treatments (Fig. 4E and F, Table S3). Taken together, these results indicate that in our laboratory population, PaMyr1 is responsible for myrosinase activity in adults, whereas PaMyr2 is mainly responsible for myrosinase activity in larvae.

3.5. PaMyr2 protects larvae against a generalist predator

To test the hypothesis that myrosinase activity protects larvae against predators, we exposed *PaMyr2*-silenced and control larvae to the generalist predator *H. axyridis*. As expected, control larvae survived significantly longer than *PaMyr2*-silenced larvae with reduced myrosinase activity ($N = 68–72$, log-rank test; experiment day, $\chi^2 = 4.5$, $P = 0.107$; dsRNA treatment, $\chi^2 = 21.8$, $P < 0.001$, Tables S3 and S6, Fig. 5A).

3.6. PaMyr2 is involved in endogenous metabolism of sequestered glucosinolates

The observation that *PaMyr2*-silenced larvae sequestered more GSL than control larvae suggested that PaMyr2 metabolizes sequestered glucosinolates also independently of predation (Fig. 4C). To test this hypothesis, we fed *PaMyr2*-silenced and control larvae with myrosinase-deficient leaves of the *A. thaliana tgg1×tgg2* mutant, and quantified the proportion of hydrolysis products in bodies and feces relative to the total amounts of 4MSOB GSL and its hydrolysis products. Bodies of *PaMyr2*-silenced larvae contained significantly less GSL hydrolysis products than bodies of control larvae (Mann-Whitney Rank sum test, $N = 12$, $U = 30$, $P = 0.017$, Table S6, Fig. 5B), whereas the proportion of GSL hydrolysis products in feces did not differ between treatments (*t*-test, $N = 12$, $t = 0.248$, $P = 0.804$, Fig. 5B). These results support the hypothesis that *PaMyr2* is not only involved in activated defense but also in endogenous GSL metabolism in *P. armoraciae* larvae.

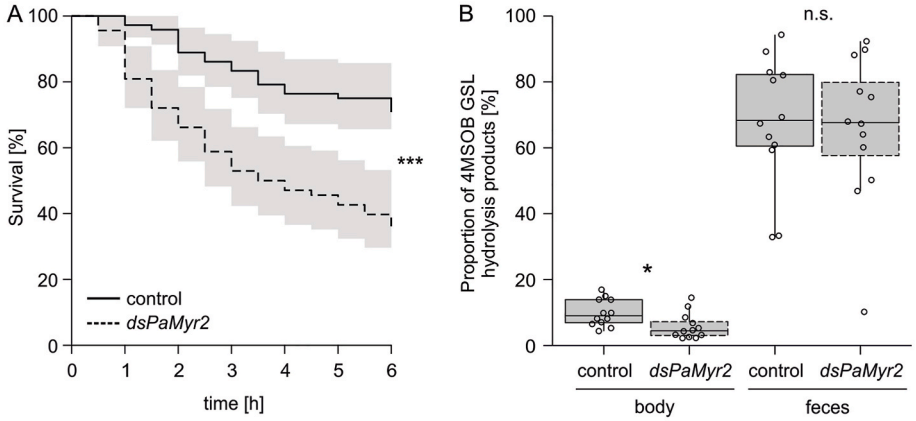

Fig. 5. PaMyr2 protects *P. armoraciae* larvae against a generalist predator and metabolizes sequestered glucosinolates in uninjured larvae. **(A)** *PaMyr2*-silenced (*dsPaMyr2*) and control larvae were exposed to the generalist predator *Harmonia axyridis*. Larval survival was monitored every 30 min for 6 h ($N = 68–72$, log-rank test, shaded area corresponds to 95% confidence interval). **(B)** *PaMyr2*-silenced (*dsPaMyr2*) and control larvae were fed for one day with leaves of the *Arabidopsis thaliana tgg1*×*tgg2* mutant, which is devoid of myrosinase activity in leaves. Afterwards, larval bodies and feces were extracted and the amounts of 4-methylsulfinyl butyl glucosinolate (4MSOB GSL) and its hydrolysis products were quantified using LC-MS/MS. The proportion of hydrolysis products was expressed relative to the total amount of detected 4MSOB GSL and hydrolysis products, which was set to 100% ($N = 12$). Box plots show the median and interquartile range of each dataset. ***, $P < 0.001$; *, $P = 0.017$; n.s., not significant.

Table 1
Glucosinolate composition in *B. rapa* plants and different life stages of *P. armoraciae*. The proportion of each GSL was calculated relative to total GSL amount (set to 1).

Glucosinolate (GSL)	Mean GSL proportion ± SD			
	B. rapa	Larvae	Pupa	Adults
	($N = 6$)	($N = 20$)	($N = 20$)	($N = 20$)
3-Butenyl GSL	0.14 ± 0.12	0.01 ± 0.08	0.02 ± 0.06	0.18 ± 0.05
4-Pentenyl GSL	0.19 ± 0.10	0.03 ± 0.08	0.05 ± 0.04	0.20 ± 0.06
2OH3But GSL	0.22 ± 0.09	0.50 ± 0.14	0.49 ± 0.08	0.32 ± 0.08
2OH4Pent GSL	0.04 ± 0.05	0.04 ± 0.03	0.06 ± 0.03	0.05 ± 0.03
5MSOP GSL	0.07 ± 0.04	0.28 ± 0.08	0.24 ± 0.07	0.10 ± 0.02
Benzyl GSL	0.07 ± 0.02	0.03 ± 0.01	0.02 ± 0.01	0.04 ± 0.01
2 PE GSL	0.01 ± 0.01	0.01 ± 0.02	0.02 ± 0.02	0.03 ± 0.01
I3M GSL	0.04 ± 0.02	0.02 ± 0.01	0.04 ± 0.02	0.04 ± 0.01
4MOI3M GSL	0.01 ± 0.01	0.01 ± 0.01	0.01 ± 0.00	0.01 ± 0.00
1MOI3M GSL	0.20 ± 0.12	0.08 ± 0.05	0.04 ± 0.02	0.02 ± 0.01

2OH3But, 2-hydroxy-3-butenyl; 2OH4Pent, 2-hydroxy-4-pentenyl; 5MSOP, 5-methylsulfinylpentyl; 2 PE, 2-phenylethyl; I3M, indol-3-ylmethyl; 4OHI3M, 4-hydroxyindol-3-ylmethyl; 4MOI3M, 4methoxyindol-3-ylmethyl; 1MOI3M, 1-methoxyindol-3-ylmethyl.

3.7. GSL sequestration patterns differ between P. armoraciae life stages

Since the substrate preference of the larval myrosinase (PaMyr2) differs from that of the adult myrosinase (PaMyr1), we asked whether these life stages also have different GSL sequestration patterns. To answer this question, we compared the GSL composition in *B. rapa* with that in *P. armoraciae* larvae, pupae, and adults (Table 1; Fig. 6; Table S7). While all GSLs detected in *B. rapa* were also detected in *P. armoraciae*, their composition differed between all life stages and, in addition, from that in their food plant (Table 1; PERMANOVA, $F = 40.906$, $P < 0.001$). In general, *P. armoraciae* contained higher proportions of 2-hydroxy-3-butenyl GSL and 5-methylsulfinylpentyl GSL, and less 1-methoxy-indol-3-ylmethyl GSL and benzyl GSL than *B. rapa*. Focusing on beetle life stages, we found that adults sequestered more 3-butenyl GSL, 4-pentenyl GSL and 2-phenylethyl GSL compared to larvae (Fig. 6). These results show that larvae and adults selectively sequester GSL from their food plant and have different sequestration patterns.

4. Discussion

Here, we identified three genes that encode enzymes with myrosinase activity in the horseradish flea beetle, *P. armoraciae* (Fig. 1). The three myrosinase genes differ in their life stage-specific expression patterns, with *PaMyr1* being mainly expressed in pupae and adults, and *PaMyr2* and *PaMyr3* being mainly expressed in eggs and larvae (Fig. 3). However, the much lower transcript levels of *PaMyr3* compared to *PaMyr2* suggest that *PaMyr3* plays only a minor role in our laboratory population of *P. armoraciae*. In fact, we later discovered that most individuals in our laboratory population do not express *PaMyr3* at all because this gene is not present in their genome. The underlying myrosinase gene copy number polymorphism was discovered in both natural and laboratory populations of *P. armoraciae* and will be presented in a follow-up study. Knockdown of *PaMyr1* in adults and *PaMyr2* in larvae reduced myrosinase activity in these life stages by more than 65% compared to the corresponding controls, suggesting that these two genes are mainly responsible for myrosinase activity in this *P. armoraciae* population (Fig. 4).

Previous research identified a single myrosinase gene in *P. striolata* using proteomic and transcriptomic data derived from adult beetles (Beran et al., 2014). It was therefore initially surprising to find several myrosinases in *P. armoraciae*. However, homology-based searches in publicly available genome sequences from *P. striolata* and *P. cruciferae* revealed that both species likely possess two myrosinase genes (Fig. 1). A possible explanation why the second putative myrosinase in *P. striolata* was not found in the previous study could be that this gene is specifically expressed in the larval stage, which was not previously analyzed. Further research is needed to verify the function of these additional candidate myrosinases in *P. striolata* and *P. cruciferae*, and to determine whether, similar to *P. armoraciae*, these genes differ in their life stage-specific expression patterns.

Our phylogenetic analyses of characterized and candidate myrosinases from *Phyllotreta* spp. predicts that the initial gene duplication event took place in a common ancestor of *P. armoraciae*, *P. striolata,* and *P. cruciferae*. Although the phylogenetic relationships within the genus *Phyllotreta* are unresolved, this points towards an early diversification of myrosinase genes in *Phyllotreta* flea beetles. Considering the high sequence similarity of *PaMyr2* and *PaMyr3* (93% nt sequence identity), it seems likely that these two genes are the result of a recent duplication in *P. armoraciae*. However, more comprehensive analyses of the myrosinase gene family in *Phyllotreta* flea beetles are needed to understand

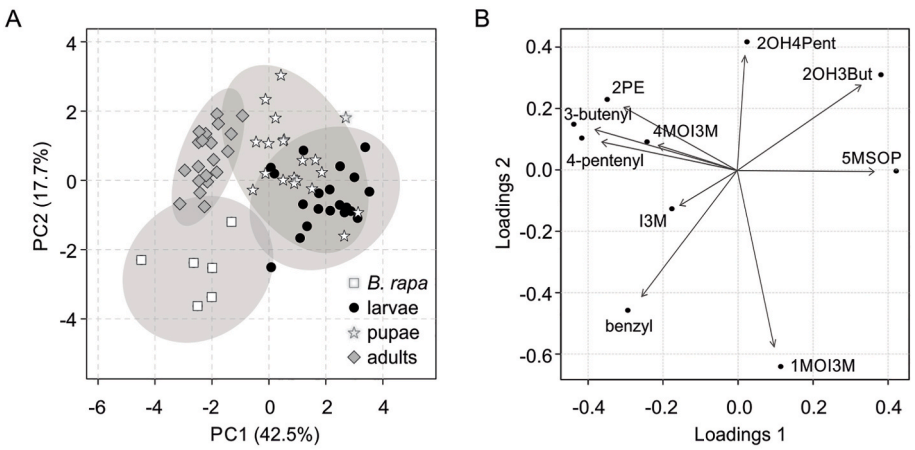

Fig. 6. Comparison of the glucosinolate composition in *B. rapa* plants and different life stages of *P. armoraciae*. Glucosinolates (GSLs) were extracted from feeding-damaged *B. rapa* leaves ($N = 6$) and different *P. armoraciae* life stages ($N = 20$ per life stage) and quantified using HPLC-DAD. The proportion of each GSL was calculated relative to total GSL amount in each sample (set to 1). **(A)** Principal component analysis (PCA) of the GSL composition in *B. rapa* and *P. armoraciae* life stages. Each symbol represents the relative GSL composition in one replicate. The ellipsoids correspond to the 95% confidence intervals of each group. **(B)** PCA loadings plot showing the contribution of the individual GSL to the separation of the samples in the PCA. 2OH3But, 2-Hydroxy-3-butenyl; 2OH4Pent, 2-Hydroxy-4-pentenyl; 5MSOP, 5-methylsulfinylpentyl; I3M, indol-3-ylmethyl; 4MOI3M, 4-methoxyindol-3-ylmethyl; 1MOI3M, 1-methoxyindol-3-ylmethy; 2 PE, 2-phenylethyl.

its evolutionary origin and dynamics.

As the name horseradish flea beetle suggests, this species is mainly associated with horseradish, *Armoraciae rusticana* (Rheinheimer and Hassler, 2018; Vig and Verdyck, 2001), in which 2-propenyl GSL constitutes more than 90% of the total GSL content in both above- and belowground plant tissues (Agneta et al., 2014; Ciska et al., 2017; Li and Kushad, 2004). Accordingly, both larvae and adults sequester predominantly 2-propenyl GSL in nature, which correlates with the substrate preferences of recombinant PaMyr1 and PaMyr3, but not with the substrate preference of PaMyr2 (Fig. 2). Considering that *P. armoraciae* larvae and adults sequester the same GSLs, it is unclear why they possess myrosinases with different biochemical properties (Fig. S3). However, the larvae of many other *Phyllotreta* species feed on plant roots and thus utilize a different plant tissue than adults, which feed on above-ground plant tissues (Rheinheimer and Hassler, 2018; Vig, 2005; Vig and Verdyck, 2001). Since the GSL composition of roots and above-ground tissues often differs (Ben Ammar et al., 2023; Ciska et al., 2017; Li and Kushad, 2004; van Dam et al., 2009), it is likely that larvae and adults of other *Phyllotreta* species also differ in their GSL composition. These chemical differences in turn may have selected for different enzyme activities in these two life stages. This hypothesis needs to be tested in studies with *Phyllotreta* species that have root-feeding larvae such as *P. striolata* and *P. cruciferae* and that likely also each possess two myrosinases (Fig. 1, Fig. S1). In addition, the different biochemical properties of myrosinase activity in larvae and adults may allow them to differentially utilize sequestered GSL for defense and/or endogenous metabolism.

Previous studies with *P. striolata* adults and cabbage aphids showed that both species selectively sequester host plant GSL, which are preferred substrates of their endogeneous myrosinase (Beran et al., 2014; Sun et al., 2021). Although the GSL sequestration pattern of *P. armoraciae* larvae differed from that of adults (Table 1, Fig. 6), these patterns only partially matched the substrate specificities of the corresponding myrosinases. For example, larvae did not accumulate more benzyl GSL than adults, but adults sequestered more 3-butenyl GSL compared to larvae. These results show that *P. armoraciae* larvae and adults differ not only in myrosinase activity but also in the sequestration of host plant GSLs, but the causes and consequences of these differences remain unknown.

In plants and insects, myrosinase-catalyzed GSL hydrolysis has mainly been considered as an activated chemical defense (Jeschke et al., 2016a; Kazana et al., 2007; Sporer et al., 2020). This view has been challenged by a number of studies with the model plant *Arabidopsis thaliana*, which have demonstrated different functions of myrosinase-catalyzed GSL degradation under both biotic and abiotic stress (Sugiyama and Hirai, 2019; Sugiyama et al., 2021). For example, under sulfur deficiency, GSLs are hydrolyzed by specific β-glucosidases to reallocate sulfur for cysteine biosynthesis, showing that GSLs also represent a sulfur reservoir for primary metabolism (Sugiyama et al., 2021). Here, we provide evidence that the beetle myrosinase PaMyr2 not only protects *P. armoraciae* larvae against a generalist predator, but is also involved in the endogenous turnover of sequestered GSL in uninjured larvae (Fig. 5). Similar to plants, this endogenous GSL turnover could also play a role in insect nutrition or pathogen defense.

The products of the endogenous GSL turnover were simple nitriles in addition to isothiocyanates and isothiocyanate-derived metabolites. In experiments with recombinant PaMyr enzymes, the formation of simple nitriles was dependent on the presence of Fe(II) ion, suggesting that Fe (II) ion and/or other factors influence the outcome of GSL hydrolysis in *P. armoraciae in vivo*. Similar to our findings, hydrolysis of sequestered GSL in cabbage aphids upon simulated predation also yielded both nitrile and isothiocyanate hydrolysis products, with nitrile formation being dependent on the presence of Fe(II) ion (Sun et al., 2021). Because simple nitriles are known to be much less reactive compared to isothiocyanates, the formation of nitriles could be a mechanism to prevent autotoxicity.

In conclusion, we have shown that different genes are responsible for myrosinase activity in *P. armoraciae* larvae and adults, leading to differences in the biochemical properties of myrosinase activity in the two life stages. Although the ecological significance of these biochemical differences remains unclear, our results highlight the importance of studying different life stages to understand the molecular basis of chemical defense strategies in insects. The roles of myrosinase activity in activated defense and endogenous glucosinolate turnover further indicate that sequestered chemical defense compounds may have multiple functions in the organism.

Author contributions

JK, TS, ZLY, and FB designed the study; JK, KO, TS, and FB performed experiments; JK, KO, TS, ZLY, and FB analyzed data, JK and FB wrote the manuscript. All authors commented and approved the submitted manuscript.

Data availability statement

The sequences reported in this paper have been deposited in the GenBank database (accession nos. OP313699 to OP313730). The raw data underlying the figures and tables are available in Edmond (the open access data repository of the Max Planck Society) under https://doi.org/10.17617/3.693PSJ.

Declaration of competing interest

None.

Acknowledgements

We thank Michael Reichelt for help with chemical analyses, Grit Kunert and Heiko Vogel for providing pea aphids and Asian lady beetles, Tobias Köllner for helpful discussions, Susanne Donnerhacke for excellent technical assistance, Domenica Schnabelrauch for Sanger sequencing service, the greenhouse team for providing plants for insect culture and experiments, and Alexander Schilling and Paula Lampe for help with the insect rearing. We also would like to thank Martin Kaltenpoth, Jonathan Gershenzon, and David G. Heckel for supporting the project in various ways. This project was funded by the Max Planck Society. Franziska Beran was supported by the DFG [grant project number 501638262].

Appendix A. Supplementary data

Supplementary data to this article can be found online at https://doi.org/10.1016/j.ibmb.2023.104040.

References

Agerbirk, N., Olsen, C.E., 2012. Glucosinolate structures in evolution. Phytochemistry 77, 16–45. https://doi.org/10.1016/j.phytochem.2012.02.005.

Agneta, R., Lelario, F., De Maria, S., Mollers, C., Bufo, S.A., Rivelli, A.R., 2014. Glucosinolate profile and distribution among plant tissues and phenological stages of field-grown horseradish. Phytochemistry 106, 178–187. https://doi.org/10.1016/j.phytochem.2014.06.019.

Almagro Armenteros, J.J., Tsirigos, K.D., Sønderby, C.K., Petersen, T.N., Winther, O., Brunak, S., von Heijne, G., Nielsen, H., 2019. SignalP 5.0 improves signal peptide predictions using deep neural networks. Nat. Biotechnol. 37, 420–423. https://doi.org/10.1038/s41587-019-0036-z.

Barth, C., Jander, G., 2006. *Arabidopsis* myrosinases TGG1 and TGG2 have redundant function in glucosinolate breakdown and insect defense. Plant J. 46, 549–562. https://doi.org/10.1111/j.1365-313X.2006.02716.x.

Ben Ammar, H., Arena, D., Treccarichi, S., Di Bella, M.C., Marghali, S., Ficcadenti, N., Lo Scalzo, R., Branca, F., 2023. The effect of water stress on the glucosinolate content and profile: a comparative study on roots and leaves of *Brassica oleracea* L. crops. Agronomy 13, 579. https://doi.org/10.3390/agronomy13020579.

Beran, F., Pauchet, Y., Kunert, G., Reichelt, M., Wielsch, N., Vogel, H., Reinecke, A., Svatos, A., Mewis, I., Schmid, D., Ramasamy, S., Ulrichs, C., Hansson, B.S., Gershenzon, J., Heckel, D.G., 2014. *Phyllotreta striolata* flea beetles use host plant defense compounds to create their own glucosinolate-myrosinase system. Proc. Natl. Acad. Sci. USA 111, 7349–7354. https://doi.org/10.1073/pnas.1321781111.

Beran, F., Petschenka, G., 2022. Sequestration of plant defense compounds by insects: from mechanisms to insect plant coevolution. Annu. Rev. Entomol. 67, 163–180. https://doi.org/10.1146/annurev-ento-062821-062319.

Beran, F., Rahfeld, P., Luck, K., Nagel, R., Vogel, H., Wielsch, N., Irmisch, S., Ramasamy, S., Gershenzon, J., Heckel, D.G., Köllner, T.G., 2016. Novel family of terpene synthases evolved from trans-isoprenyl diphosphate synthases in a flea beetle. Proc. Natl. Acad. Sci. USA 113, 2922–2927. https://doi.org/10.1073/pnas.1523468113.

Blažević, I., Montaut, S., Burčul, F., Olsen, C.E., Burow, M., Rollin, P., Agerbirk, N., 2020. Glucosinolate structural diversity, identification, chemical synthesis and metabolism in plants. Phytochemistry 169. https://doi.org/10.1016/j.phytochem.2019.112100.

Chhajed, S., Misra, B.B., Tello, N., Chen, S.X., 2019. Chemodiversity of the glucosinolate-myrosinase system at the single cell type resolution. Front. Plant Sci. 10 https://doi.org/10.3389/fpls.2019.00618.

Ciska, E., Horbowicz, M., Rogowska, M., Kosson, R., Drabinska, N., Honke, J., 2017. Evaluation of seasonal variations in the glucosinolate content in leaves and roots of four European horseradish (*Armoracia rusticana*) landraces. Polish J. Food. 67, 301–308. https://doi.org/10.1515/pjfns-2016-0029.

de Castro, É.C.P., Zagrobelny, M., Zurano, J.P., Zikan Cardoso, M., Feyereisen, R., Bak, S., 2019. Sequestration and biosynthesis of cyanogenic glucosides in passion vine butterflies and consequences for the diversification of their host plants. Ecol. Evol. 9, 5079–5093. https://doi.org/10.1002/ece3.5062.

Dettner, K., 2015. Toxins, defensive compounds and drugs from insects. In: Hoffmann, K. H. (Ed.), Insect Molecular Biology and Ecology. CRC Press, Taylor & Francis Group, LLC, Boca Raton, London, New York, pp. 39–93.

Eisenschmidt-Bönn, D., Schneegans, N., Backenkohler, A., Wittstock, U., Brand, W., 2019. Structural diversification during glucosinolate breakdown: mechanisms of thiocyanate, epithionitrile and simple nitrile formation. Plant J. 99, 329–343. https://doi.org/10.1111/tpj.14327.

Gasteiger, E., Hoogland, C., Gattiker, A., Duvaud, S., Wilkins, M.R., Appel, R.D., Bairoch, A., 2005. Protein identification and analysis tools on the ExPASy Server. In: Walker, J.M. (Ed.), The Proteomics Protocols Handbook. Humana Press, Totowa, NJ, pp. 571–607.

Gikonyo, M.W., Biondi, M., Beran, F., 2019. Adaptation of flea beetles to Brassicaceae: host plant associations and geographic distribution of *Psylliodes* Latreille and *Phyllotreta* Chevrolat (Coleoptera, Chrysomelidae). In: Schmitt, M., Chaboo, C.S., Biondi, M. (Eds), Research on Chrysomelidae 8. ZooKeys 856, pp. 51-73. https://doi.org/10.3897/zookeys.856.33724.

Gupta, R., Brunak, S., 2002. Prediction of glycosylation across the human proteome and the correlation to protein function. Pacific Symposium on Biocomputing 310–322.

Haldane, J.B.S., 1930. Enzymes. Longmans, Green, London.

Hanschen, F.S., Lamy, E., Schreiner, M., Rohn, S., 2014. Reactivity and stability of glucosinolates and their breakdown products in foods. Angew. Chem. Int. Ed. 53, 11430–11450. https://doi.org/10.1002/anie.201402639.

He, S., Jiang, B., Chakraborty, A., Yu, G., 2022. The evolution of Glycoside Hydrolase Family 1 in insects related to their adaptation to plant utilization. Insects 13, 786. https://doi.org/10.3390/insects13090786.

Hoang, D.T., Chernomor, O., von Haeseler, A., Minh, B.Q., Vinh, L.S., 2018. UFBoot2: improving the ultrafast bootstrap approximation. Mol. Biol. Evol. 35, 518–522. https://doi.org/10.1093/molbev/msx281.

Hothorn, T., Bretz, F., Westfall, P., 2020. multcomp: simultaneous inference in general parametric models. R package version 1, 4–14.

Huelsenbeck, J.P., Ronquist, F., 2001. MRBAYES: Bayesian inference of phylogenetic trees. Bioinformatics 17, 754–755. https://doi.org/10.1093/bioinformatics/17.8.754.

Jeschke, V., Gershenzon, J., Vassão, D.G., 2016a. Insect detoxification of glucosinolates and their hydrolysis products. In: Kopriva, S. (Ed.), Advances in Botanical Research: Glucosinolates. Elsevier, UK, pp. 199–245.

Jeschke, V., Gershenzon, J., Vassão, D.G., 2016b. A mode of action of glucosinolate-derived isothiocyanates: Detoxification depletes glutathione and cysteine levels with ramifications on protein metabolism in *Spodoptera littoralis*. Insect Biochem. Mol. Biol. 71, 37–48. https://doi.org/10.1016/j.ibmb.2016.02.002.

Jones, A.M., Bridges, M., Bones, A.M., Cole, R., Rossiter, J.T., 2001. Purification and characterisation of a non-plant myrosinase from the cabbage aphid *Brevicoryne brassicae* (L.). Insect Biochem. Mol. Biol. 31, 1–5. https://doi.org/10.1016/s0965-1748(00)00157-0.

Kalyaanamoorthy, S., Minh, B.Q., Wong, T.K.F., von Haeseler, A., Jermiin, L.S., 2017. ModelFinder: fast model selection for accurate phylogenetic estimates. Nat. Methods 14, 587–589. https://doi.org/10.1038/nmeth.4285.

Katoh, K., Rozewicki, J., Yamada, K.D., 2019. MAFFT online service: multiple sequence alignment, interactive sequence choice and visualization. Briefings Bioinf. 20, 1160–1166. https://doi.org/10.1093/bib/bbx108.

Kazana, E., Pope, T.W., Tibbles, L., Bridges, M., Pickett, J.A., Bones, A.M., Powell, G., Rossiter, J.T., 2007. The cabbage aphid: a walking mustard oil bomb. Proc. R. Soc. B: Biol. Sci. 274, 2271–2277. https://doi.org/10.1098/rspb.2007.0237.

King, R., Buer, B., Davies, T.G.E., Ganko, E., Guest, M., Hassani-Pak, K., Hughes, D., Raming, K., Rawlings, C., Williamson, M., Crossthwaite, A., Nauen, R., Field, L., 2023. The complete genome assemblies of 19 insect pests of worldwide importance to agriculture. Pestic. Biochem. Physiol., 105339 https://doi.org/10.1016/j.pestbp.2023.105339.

Li, X., Kushad, M.M., 2004. Correlation of glucosinolate content to myrosinase activity in horseradish (*Armoracia rusticana*). J. Agric. Food Chem. 52, 6950–6955. https://doi.org/10.1021/jf0401827.

Miller, M., Pfeiffer, W.T., Schwartz, T., 2010. Creating the CIPRES Science Gateway for Inference of Large Phylogenetic Trees.

Mumm, R., Burow, M., Bukovinszkine'Kiss, G., Kazantzidou, E., Wittstock, U., Dicke, M., Gershenzon, J., 2008. Formation of simple nitriles upon glucosinolate hydrolysis affects direct and indirect defense against the specialist herbivore, *Pieris rapae*. J. Chem. Ecol. 34, 1311–1321. https://doi.org/10.1007/s10886-008-9534-z.

Nguyen, L.-T., Schmidt, H.A., von Haeseler, A., Minh, B.Q., 2015. IQ-TREE: a fast and effective stochastic algorithm for estimating maximum-likelihood phylogenies. Mol. Biol. Evol. 32, 268–274. https://doi.org/10.1093/molbev/msu300.

Pang, Z., Chong, J., Zhou, G., de Lima Morais, D.A., Chang, L., Barrette, M., Gauthier, C., Jacques, P.-É., Li, S., Xia, J., 2021. MetaboAnalyst 5.0: narrowing the gap between raw spectra and functional insights. Nucleic Acids Res. 49, W388–W396. https://doi.org/10.1093/nar/gkab382.

Pentzold, S., Jensen, M.K., Matthes, A., Olsen, C.E., Petersen, B.L., Clausen, H., Møller, B. L., Bak, S., Zagrobelny, M., 2017. Spatial separation of the cyanogenic beta-glucosidase ZfBGD2 and cyanogenic glucosides in the haemolymph of *Zygaena* larvae facilitates cyanide release. R. Soc. Open Sci. 4, 13. https://doi.org/10.1098/rsos.170262.

Pinheiro, J., Bates, D., DebRoy, S., Sarkar, D., Team, R.C., 2021. nlme: linear and nonlinear mixed effects models. R package version 3, 1–153.

Pontoppidan, B., Ekbom, B., Eriksson, S., Meijer, J., 2001. Purification and characterization of myrosinase from the cabbage aphid (*Brevicoryne brassicae*), a

brassica herbivore. Eur. J. Biochem. 268, 1041–1048. https://doi.org/10.1046/j.1432-1327.2001.01971.x.
R Core Team, 2023. R: A Language and Environment for Statistical Computing. R foundation for statistical computing, Vienna, Austria. Available at: http://www.r-project.org/.
Rahfeld, P., Haeger, W., Kirsch, R., Pauls, G., Becker, T., Schulze, E., Wielsch, N., Wang, D., Groth, M., Brandt, W., Boland, W., Burse, A., 2015. Glandular beta-glucosidases in juvenile Chrysomelina leaf beetles support the evolution of a host-plant-dependent chemical defense. Insect Biochem. Mol. Biol. 58, 28–38. https://doi.org/10.1016/j.ibmb.2015.01.003.
Rheinheimer, J., Hassler, M., 2018. Die Blattkäfer Baden-Württembergs. Kleinsteuber Books, Karlsruhe, Germany.
Ritz, C., Baty, F., Streibig, J.C., Gerhard, D., 2015. Dose-response analysis using R. PLoS One 10. https://doi.org/10.1371/journal.pone.0146021.
Robert, C.A.M., Zhang, X., Machado, R.A.R., Schirmer, S., Lori, M., Mateo, P., Erb, M., Gershenzon, J., 2017. Sequestration and activation of plant toxins protect the western corn rootworm from enemies at multiple trophic levels. eLife 6, 17. https://doi.org/10.7554/eLife.29307.
Ronquist, F., Teslenko, M., van der Mark, P., Ayres, D.L., Darling, A., Höhna, S., Larget, B., Liu, L., Suchard, M.A., Huelsenbeck, J.P., 2012. MrBayes 3.2: efficient Bayesian phylogenetic inference and model choice across a large model space. Syst. Biol. 61, 539–542. https://doi.org/10.1093/sysbio/sys029.
Scanlon, J.T., Willis, D.E., 1985. Calculation of flame ionization detector relative response factors using the effective carbon number concept. J. Chromatogr. Sci. 23, 333–340. https://doi.org/10.1093/chromsci/23.8.333.
Sonnad, J.R., Goudar, C.T., 2004. Solution of the Haldane equation for substrate inhibition enzyme kinetics using the decomposition method. Math. Comput. Model. 40, 573–582. https://doi.org/10.1016/j.mcm.2003.10.051.
Spencer, G.F., 1980. Gas chromatography-mass spectrometry of nitriles, isothiocyanates and oxazolidinethiones derived from cruciferous glucosinolates. J. Sci. Food Agric. 31, 359–367. https://doi.org/10.1002/jsfa.2740310406, 1980 v.1931 no.1984.
Sporer, T., Körnig, J., Beran, F., 2020. Ontogenetic differences in the chemical defence of flea beetles influence their predation risk. Funct. Ecol. 34, 1370–1379. https://doi.org/10.1111/1365-2435.13548.
Sporer, T., Körnig, J., Wielsch, N., Gebauer-Jung, S., Reichelt, M., Hupfer, Y., Beran, F., 2021. Hijacking the mustard-oil bomb: how a glucosinolate-sequestering flea beetle copes with plant myrosinases. Front. Plant Sci. 12, 645030 https://doi.org/10.3389/fpls.2021.645030.
Sugiura, S., 2020. Predators as drivers of insect defenses. Entomol. Sci. 23, 316–337. https://doi.org/10.1111/ens.12423.
Sugiyama, R., Hirai, M.Y., 2019. Atypical myrosinase as a mediator of glucosinolate functions in plants. Front. Plant Sci. 10 https://doi.org/10.3389/fpls.2019.01008.
Sugiyama, R., Li, R., Kuwahara, A., Nakabayashi, R., Sotta, N., Mori, T., Ito, T., Ohkama-Ohtsu, N., Fujiwara, T., Saito, K., Nakano, R.T., Bednarek, P., Hirai, M.Y., 2021. Retrograde sulfur flow from glucosinolates to cysteine in *Arabidopsis thaliana*. Proc. Natl. Acad. Sci. USA 118. https://doi.org/10.1073/pnas.2017890118.
Sun, R., Jiang, X.C., Reichelt, M., Gershenzon, J., Vassão, D.G., 2021. The selective sequestration of glucosinolates by the cabbage aphid severely impacts a predatory lacewing. J. Pest. Sci. 94, 1147–1160. https://doi.org/10.1007/s10340-020-01319-2.
Talavera, G., Castresana, J., 2007. Improvement of phylogenies after removing divergent and ambiguously aligned blocks from protein sequence alignments. Syst. Biol. 56, 564–577. https://doi.org/10.1080/10635150701472164.
Therneau, T.M., 2020. A Package for Survival Analysis in R. R Package Version 3, pp. 1–12.
Thies, W., 1988. Isolation of sinigrin and glucotropaeolin from cruciferous seeds. Fat Sci. Technol. 90, 311–314. https://doi.org/10.1002/lipi.19880900806.
van Dam, N.M., Tytgat, T.O.G., Kirkegaard, J.A., 2009. Root and shoot glucosinolates: a comparison of their diversity, function and interactions in natural and managed ecosystems. Phytochemistry Rev. 8, 171–186. https://doi.org/10.1007/s11101-008-9101-9.
Vig, K., 2005. Biology of *Phyllotreta* (Alticinae), with Emphasis on Hungarian and Middle European Species. In: Jolivet, P., Santiago-Blay, J., Schmitt, M. (Eds.), New Developments in the Biology of Chrysomelidae. Brill, The Hague, The Netherlands, pp. 565–576.
Vig, K., Verdyck, P., 2001. Data on the host plant selection of the horseradish flea beetle, *Phyllotreta armoraciae* (Koch, 1803) (Coleoptera, Chrysomelidae, Alticinae). Meded Rijksuniv Gent Fak Landbouwkd Toegep Biol Wet 66, 277–283.
Wittstock, U., Kurzbach, E., Herfurh, A.-M., Stauber, E.J., 2016. Glucosinolate breakdown. In: Kopriva S. (Ed), Advances in Botanical Research: Glucosinolates. Elsevier, UK, pp. 125–169.
Yang, Z.L., Kunert, G., Sporer, T., Körnig, J., Beran, F., 2020. Glucosinolate abundance and composition in Brassicaceae influence sequestration in a specialist flea beetle. J. Chem. Ecol. 46 https://doi.org/10.1007/s10886-020-01144-y.
Yang, Z.L., Nour-Eldin, H.H., Hänniger, S., Reichelt, M., Crocoll, C., Seitz, F., Vogel, H., Beran, F., 2021. Sugar transporters enable a leaf beetle to accumulate plant defense compounds. Nat. Commun. 12 https://doi.org/10.1038/s41467-021-22982-8.
Zagrobelny, M., de Castro É, C.P., Møller, B.L., Bak, S., 2018. Cyanogenesis in Arthropods: from chemical warfare to nuptial gifts. Insects 9. https://doi.org/10.3390/insects9020051.
Zuur, A.F., 2009. Mixed Effects Models and Extensions in Ecology with R. Springer, New York, NY.
Benjamini, Y., Yekutieli, D., 2001. The control of the false discovery rate in multiple testing under dependency. The Annals of Statistics 29, 1165–1188. https://doi.org/10.1214/aos/1013699998.
Kindt, R., Coe, R., 2005. Tree diversity analysis. A manual and software for common statistical methods for ecological and biodiversity studies. Nairobi: World Agroforestry Centre (ICRAF). World Agroforestry Centre, Nairobi, Kenya.
Oksanen, J.S.G., Blanchet, F., Kindt, R., Legendre, P., Minchin, P., O'Hara, R., Solymos, P., Stevens, M., Szoecs, E., Wagner, H., Barbour, M., Bedward, M., Bolker, B.B.D., Carvalho, G., Chirico, M., De Caceres, M., Durand, S., Evangelista, H., FitzJohn, R., Friendly, M., Furneaux, B., Hannigan, G., Hill, M., Lahti, L.M.D., Ouellette, M., Ribeiro Cunha, E., Smith, T., Stier, A., Ter Braak, C., Weedon, J., 2022. vegan: Community Ecology Package. R package version 2.5-7. 2020. https://CRAN.R-project.org/package=vegan.